Aminoacrylate Intermediates in the Reaction of *Citrobacter freundii* Tyrosine Phenol-Lyase†

Robert S. Phillips,*,‡,§ Hao Yuan Chen,§ and Nicolai G. Faleev||

Departments of Chemistry and of Biochemistry and Molecular Biology, University of Georgia, Athens, Georgia 30602-2556, and Nesmeyanov Institute of Organoelement Compounds, Russian Academy of Sciences, 28 Vavilov Street, Moscow 117813, Russia

Received March 21, 2006; Revised Manuscript Received June 1, 2006

ABSTRACT: Tyrosine phenol-lyase (TPL) from *Citrobacter freundii* is a pyridoxal 5′-phosphate (PLP)-dependent enzyme that catalyzes the reversible hydrolytic cleavage of L-Tyr to give phenol and ammonium pyruvate. The proposed reaction mechanism for TPL involves formation of an external aldimine of the substrate, followed by deprotonation of the α-carbon to give a quinonoid intermediate. Elimination of phenol then has been proposed to give an α-aminoacrylate Schiff base, which releases iminopyruvate that ultimately undergoes hydrolysis to yield ammonium pyruvate. Previous stopped-flow kinetic experiments have provided direct spectroscopic evidence for the formation of the external aldimine and quinonoid intermediates in the reactions of substrates and inhibitors; however, the predicted α-aminoacrylate intermediate has not been previously observed. We have found that 4-hydroxypyridine, a non-nucleophilic analogue of phenol, selectively binds and stabilizes aminoacrylate intermediates in reactions of TPL with *S*-alkyl-L-cysteines, L-tyrosine, and 3-fluoro-L-tyrosine. In the presence of 4-hydroxypyridine, a new absorption band at 338 nm, assigned to the α-aminoacrylate, is observed with these substrates. Formation of the 338 nm peaks is concomitant with the decay of the quinonoid intermediates, with good isosbestic points at ∼365 nm. The value of the rate constant for aminoacrylate formation is similar to k_{cat}, suggesting that leaving group elimination is at least partially rate limiting in TPL reactions. In the reaction of *S*-ethyl-L-cysteine in the presence of 4-hydroxypyridine, a subsequent slow reaction of the α-aminoacrylate is observed, which may be due to iminopyruvate formation. Both L-tyrosine and 3-fluoro-L-tyrosine exhibit kinetic isotope effects of ∼2−3 on α-aminoacrylate formation when the α-^{2}H-labeled substrates are used, consistent with the previously reported internal return of the α-proton to the phenol product. These results are the first direct spectroscopic observation of α-aminoacrylate intermediates in the reactions of TPL.

Tyrosine phenol-lyase (TPL,[1] EC 4.1.99.2) is a pyridoxal 5′-phosphate (PLP)-dependent enzyme that catalyzes the hydrolytic cleavage of L-tyrosine to yield phenol and ammonium pyruvate (eq 1).

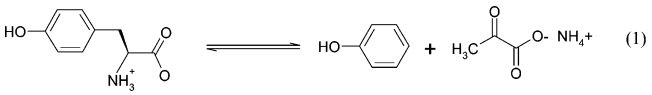

(1)

This enzymatic β-elimination of a carbon leaving group is mechanistically interesting, since the elimination cleaves a carbon−carbon bond, and hence, the phenol ring should undergo tautomerization for the elimination reaction to proceed (*1*, *2*). In addition to the physiological reaction, TPL also efficiently catalyzes the β-elimination of a number of β-substituted amino acids with good leaving groups, such as *S*-methyl-L-cysteine (*3*), β-chloroalanine (*3*), and *S*-(*o*-nitrophenyl)-L-cysteine (SOPC) (*4*). Moreover, TPL has been shown to catalyze the racemization of alanine, but at a rate much slower than the rate of β-elimination reactions (*5*, *6*).

A generally accepted chemical mechanism for the β-elimination reactions is shown in Scheme 1. The sequence includes the initial formation of an external aldimine, with a C═N bond between the PLP carbonyl group and the substrate amino group, α-proton abstraction to form a quinonoid intermediate, followed by β-elimination, which results in the formation of an α-aminoacrylate derivative, and, finally, release of this intermediate to form ammonium pyruvate. However, there have been only a few kinetic studies of TPL to support the postulated mechanism. Spectroscopic investigations have demonstrated the formation of external aldimine and quinonoid intermediates with substrates and inhibitors. Stopped-flow kinetic studies of TPL (*7*) have demonstrated two relaxation processes upon addition of inhibitors (L-alanine, D-alanine, and L-*m*-tyrosine) to TPL and three relaxation processes upon addition of the substrate,

† This work was partially supported by a grant from the National Institutes of Health (GM-42588) to R.S.P. and a grant from the Russian Foundation for Basic Investigation (04-04-49370) to N.G.F.

* To whom correspondence should be addressed: Department of Chemistry, University of Georgia, Athens, GA 30605-2556. Phone: (706) 542-1996. Fax: (706) 542-9454. E-mail: rsphillips@chem.uga.edu.

‡ Department of Chemistry, University of Georgia.

§ Department of Biochemistry and Molecular Biology, University of Georgia.

|| Russian Academy of Sciences.

[1] Abbreviations: TPL, tyrosine phenol-lyase (deaminating) (EC 4.1.99.2); Trpase, tryptophan indole-lyase (tryptophanase) (EC 4.1.99.1); PLP, pyridoxal 5′-phosphate; SOPC, *S*-(*o*-nitrophenyl)-L-cysteine; 4-HP, 4-hydroxypyridine.

10.1021/bi060561o CCC: $33.50
Published on Web 07/15/2006

Scheme 1

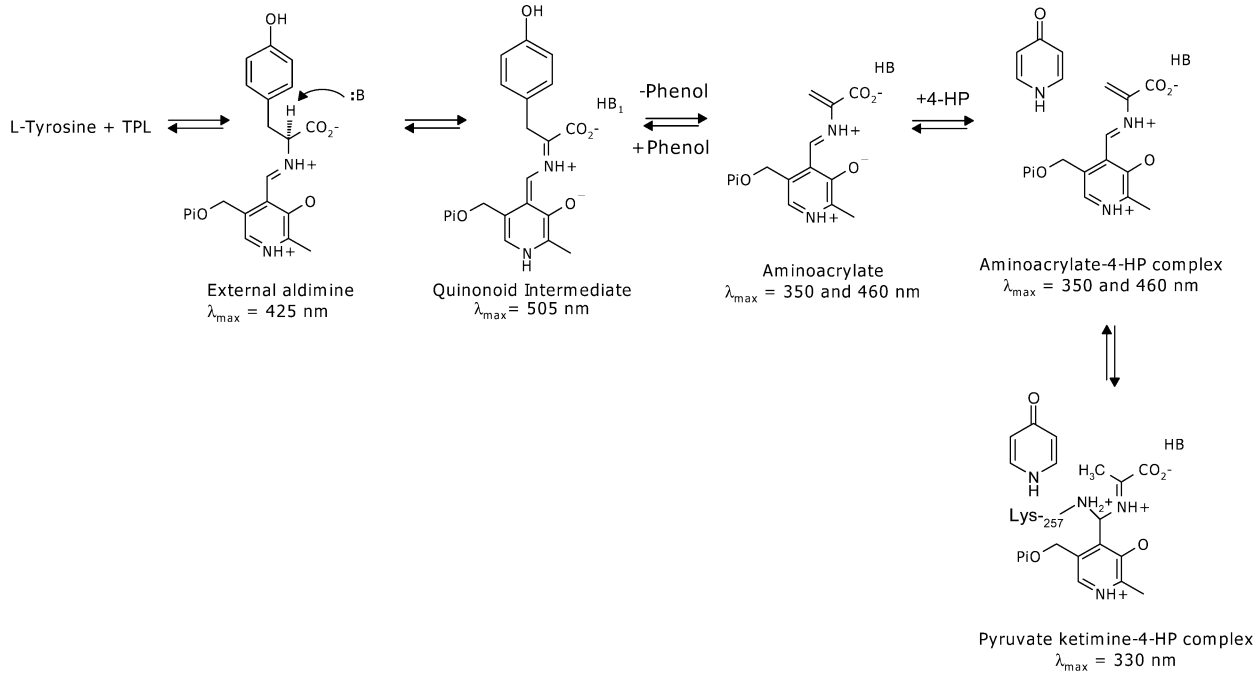

L-tyrosine. The isotope effect and pH-dependent kinetic studies of TPL (*8*) have shown that TPL appears to require two bases, one of which (pK_a = 7.6−7.8) abstracts the proton from the α-position of the substrate to form a quinonoid intermediate and the second of which (pK_a = 8.0−8.2) abstracts the proton from the substrate hydroxyl group to facilitate cyclohexadienone formation and subsequent elimination of phenol. The structure of the complex of TPL with an inhibitor, 3-(4-hydroxyphenyl)propionic acid, demonstrated that Arg-381 may be the basic residue (*9*). We have studied the steady-state and pre-steady-state kinetics of the alanine racemization catalyzed by TPL and the effects of phenol and analogues on this reaction (*6*). The results demonstrated that there are two distinct quinonoid intermediates formed from either D- or L-alanine and suggested that the interconversion of quinonoid intermediates is rate-limiting in the racemization of alanine. Thus, although external aldimine and quinonoid intermediates have been observed in the reaction of TPL with substrates and inhibitors, the postulated α-aminoacrylate intermediate shown in Scheme 1 has not been observed previously.

Tryptophan indole-lyase (tryptophanase or Trpase) is also a β-eliminating carbon−carbon lyase. Trpase from *Escherichia coli* is substantially homologous in sequence (ca. 40% identical residues) with *Citrobacter freundii* TPL (*10*). Crystallographic studies of Trpase from *Proteus vulgaris* have revealed that the three-dimensional structure of Trpase is virtually identical with that of TPL (*11*). Moreover, the proposed chemical mechanisms for TPL and Trpase are very similar (*8*, *12*). In previous studies, we have examined the effects of indole and benzimidazole on the pre-steady-state kinetics of β-elimination reactions catalyzed by Trpase (*13*−*15*). These results demonstrated the first direct measurement of the formation of an α-aminoacrylate intermediate from the breakdown of the quinonoid intermediates in the reaction of substrates with Trpase. In this study, we have studied the effects of 4-hydroxypyridine (4-HP), an analogue of phenol, on the reactions of TPL. These results provide the first direct spectroscopic evidence of transient α-aminoacrylate intermediates in the β-elimination reaction catalyzed by TPL.

MATERIALS AND METHODS

Materials. Lactate dehydrogenase (LDH) from rabbit muscle, PLP, NADH, L-tyrosine, 3-iodo-L-tyrosine, *S*-benzyl-L-cysteine, and *S*-ethyl-L-cysteine were obtained from USB Corp. *S*-Methyl-L-cysteine was a product of ICN Biochemicals. 4-Hydroxypyridine (4-HP) was obtained from Aldrich. *S*-(*o*-Nitrophenyl)-L-cysteine (SOPC) (*16*) and 3-fluoro-L-tyrosine (*17*) were prepared as previously described. [α-^{2}H]-L-Tyrosine and [α-^{2}H]-3-fluoro-L-tyrosine were prepared by performing the enzymatic synthesis reaction in 99% ^2H_2O, with phenol and 2-fluorophenol, respectively, as previously described for [α-^{2}H]-L-tyrosine (*6*, *8*). The α-^{2}H content was determined to be >98% by ^{1}H NMR for both deuterated compounds. 3-Chloro-L-tyrosine hydrochloride was obtained from Sigma. 3-Bromo-L-tyrosine was prepared in our laboratory by a new procedure (R. S. Phillips, unpublished results). All other reagents and chemicals obtained from commercially available sources were of the highest available quality.

Enzyme and Assays. Tyrosine phenol-lyase was purified from *E. coli* SVS370 cells containing pTZTPL as described previously (*18*). Enzyme concentrations were estimated from the $A_{278}^{1\%}$ of 8.37 (*7*) assuming a subunit molecular weight of 51 000 (*10*). Enzyme activity was routinely measured with 0.6 mM SOPC in 50 mM potassium phosphate (pH 8.0) at 25 °C (*4*) following the absorbance decrease at 370 nm ($\Delta\epsilon = -1.86 \times 10^3$ M^{-1} cm^{-1}). A unit of activity is defined as the amount of enzyme which produces 1 μmol of product/min at 25 °C. The activity of other substrates was measured using the coupled assay with lactate dehydrogenase and NADH, measured at 340 nm ($\Delta\epsilon = -6.22 \times 10^3$ M^{-1} cm^{-1}), as described by Morino et al. for Trpase (*19*). All the steady-state kinetic measurements were obtained on a Gilford Response or a Cary 1 UV−visible spectrophotometer equipped with a thermoelectric block. The inhibition constant

for 4-HP was determined with the FORTRAN programs of Cleland (*20*).

Rapid Reactions. Rapid-scanning stopped-flow experiments were performed on an OLIS RSM-1000 instrument, equipped with a stopped-flow mixer with a 1 cm path length. The dead time of the stopped-flow mixer is ~2 ms. Single-wavelength stopped-flow experiments were performed with a Kinetics Instruments stopped-flow mixer with a modified Cary 14 UV−visible spectrophotometer from OLIS for the light source. Prior to performing the rapid kinetic experiments, we incubated the stock enzyme with 0.5 mM PLP for 1 h at 30 °C and then separated from excess PLP on a short desalting column (PD-10, Pharmacia) equilibrated with 50 mM potassium phosphate buffer (pH 8.0). The rapid-scanning stopped-flow kinetic measurements were performed at room temperature, which was approximately 20 °C, while the single-wavelength stopped-flow kinetic measurements were performed at 25 °C, controlled by a circulating water bath. The difference in rate constants due to the temperature difference should be a factor of <1.5, assuming an average activation energy of 15 kcal/mol. The rapid-scanning stopped-flow data were analyzed with GlobalWorks supplied by OLIS (*21*) to obtain the reported rate constants. Single-wavelength transients were analyzed by fitting with SIFIT (OLIS), which can fit up to three exponentials and an offset. The quality of the fit was judged by analysis of the residuals and by the Durbin−Watson value (*22*). Isotope effects for the reaction of deuterated substrates were determined by comparison of the rate constants for the protio and deuterio substrates. Identical isotope effects, within experimental error, were obtained using the method of Fisher (*23*), which uses the initial rates of transients rather than fitted rate constants. The concentration dependence of relaxations was fit to either eq 2 for first-order reactions preceded by a rapid binding equilibrium exhibiting a hyperbolic concentration dependence (*24*) or eq 3 for first-order reactions followed by a rapid binding equilibrium exhibiting an inverted hyperbolic concentration dependence.

$$1/\tau = k_f[L]/(K_d + [L]) + k_r \quad (2)$$

$$1/\tau = k_f + k_r K_d/(K_d + [L]) \quad (3)$$

where k_f is the rate constant for the forward reaction, k_r is the rate constant for the reverse reaction, and K_d is the equilibrium constant for the binding step.

RESULTS

Rapid-Scanning Stopped-Flow Kinetic Studies of S-Alkyl-L-cysteines. The formation of quinonoid intermediates in β-elimination reactions catalyzed by TPL can be observed by stopped-flow spectrophotometry (*6*, *7*, *25*). When TPL is mixed with 40 mM *S*-ethyl-L-Cys, the external aldimine is formed in the dead time of the instrument, which can be seen in the absorbance increase and slight blue shift of the peak of spectrum 1 in Figure 1A compared to the internal aldimine (dotted line). There is a subsequent absorbance decrease at 425 nm, and a concomitant increase at 504 nm (Figure 1A). The absorbance at 504 nm reaches a maximum value at ~50 ms and then decreases in a subsequent slow phase, which is concomitant with formation of a small shoulder at ~340 nm (Figure 1B). We have also performed

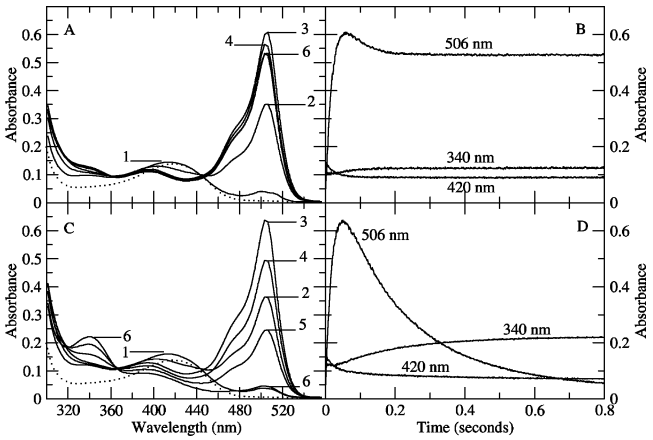

FIGURE 1: Rapid-scanning stopped-flow spectra of the reaction of TPL with *S*-ethyl-L-Cys. (A) Reaction of TPL with 40 mM *S*-ethyl-L-Cys in 0.05 M potassium phosphate (pH 8). The scans are shown at (1) 0.002, (2) 0.013, (3) 0.025, (4) 0.120, (5) 0.420, and (6) 0.920 s. (B) Time courses for the reaction shown in panel A at 340, 420, and 506 nm. (C) Reaction of TPL with 40 mM *S*-ethyl-L-Cys and 5 mM 4-HP in 0.05 M potassium phosphate (pH 8). The scans are shown at (1) 0.002, (2) 0.012, (3) 0.050, (4) 0.119, (5) 0.460, and (6) 0.920 s. (D) Time courses for the reaction shown in panel C at 340, 420, and 506 nm.

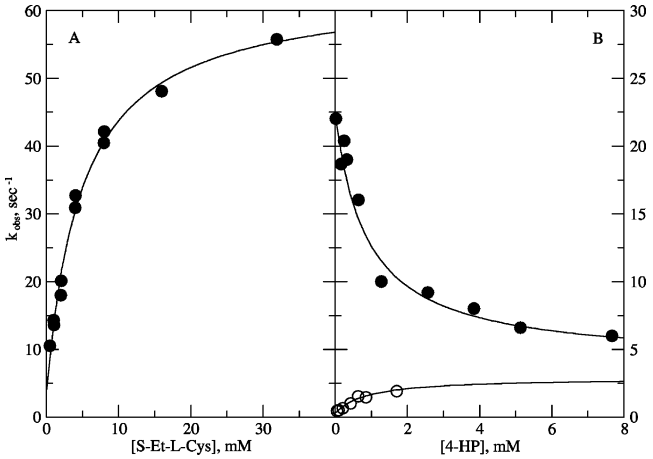

FIGURE 2: (A) Concentration dependence of the rate constant for quinonoid intermediate formation from TPL and *S*-ethyl-L-cysteine. (B) Concentration dependence of the rate constants for quinonoid intermediate decay in the reaction of TPL with *S*-ethyl-L-Cys in the presence of 4-HP: (●) fast phase and (○) slow phase.

comparable rapid-scanning stopped-flow experiments with *S*-benzyl-L-Cys and *S*-methyl-L-Cys, and similar results were obtained (data not shown).

Single-wavelength stopped-flow kinetic experiments were performed at 504 nm at various concentrations of *S*-ethyl-L-Cys. As expected from the data in Figure 1, the time courses require a minimum of two exponentials to obtain adequate fits. The rate constant for the fast phase, with an increasing absorbance, was found to increase with a hyperbolic dependence on the concentration of *S*-ethyl-L-Cys (Figure 2A). Fitting the data in Figure 2A to eq 2 gives the following: $k_f = 59.4 \pm 1.8$ s^{-1}, $k_r = 3.9 \pm 0.7$ s^{-1}, and $K_{eq} = 4.9 \pm 0.7$ mM. It could not be determined if there is a concentration dependence of the second phase, with a decreasing absorbance, because the amplitude is less than 10% of the amplitude of the first phase. The formation of quinonoid intermediates in the reactions of TPL with *S*-methyl-L-cysteine and *S*-benzyl-L-cysteine was also found

Table 1: Pre-Steady-State Kinetic Parameters for the Formation of Quinonoid Intermediates in the Reactions of TPL with *S*-Alkyl-L-cysteines

substrate	k_f (s^{-1})	k_r (s^{-1})	K_{eq} (mM)	K_d (mM)
S-methyl-L-Cys	28.1 ± 2.0	1.4 ± 0.8	21.6 ± 5.3	1.1
S-ethyl-L-Cys	59.4 ± 1.8	3.9 ± 0.7	4.9 ± 0.7	0.3
S-benzyl-L-Cys	41.1 ± 1.6	4.2 ± 0.5	1.8 ± 0.2	0.2

to exhibit a hyperbolic dependence on concentration, similar to that in Figure 2. The rate constants for deprotonation (k_f) and reprotonation (k_r) and the dissociation constants (K_{eq}) were determined by fitting the concentration-dependent data to eq 2. The results are listed in Table 1.

In previous work, we demonstrated that 4-hydroxypyridine (4-HP) can bind to the quinonoid complexes of L-alanine or D-alanine with TPL, resulting in changes in the absorption intensity (*6*). Rapid-scanning studies of the reaction of TPL with *S*-ethyl-L-Cys in the presence of 4-HP show that the quinonoid peak forms rapidly, which was seen without 4-HP, but subsequently slowly decays to a much lower absorbance value (Figure 1C,D). Formation of a peak absorbing at 338 nm is concomitant with the slow decay of the 504 nm peak, with a good isosbestic point at ~366 nm. The reaction of *S*-ethyl-L-Cys in the presence of 4-HP is triphasic (Figure 1D). The rate constant for the fast phase, with an increasing absorbance at 504 nm, is independent of 4-HP concentration but shows a dependence on *S*-ethyl-L-Cys concentration, which was seen in Figure 2A. The rate constant for the second phase, with a decreasing absorbance at 504 nm and an increasing absorbance at 338 nm, decreases with an increase in 4-HP concentration in an inverted hyperbola [Figure 2B (●)]. The rate constant for the slowest phase, with a decreasing absorbance at 504 nm, increases with 4-HP concentration in a hyperbolic manner [Figure 2B (○)]. The amplitude of this slowest phase is low, and it was not possible to fit the data for 4-HP concentration above 2 mM. Rapid-scanning stopped-flow studies of the reaction of TPL with *S*-methyl-L-Cys and *S*-benzyl-L-Cys in the presence of 4-HP show results similar to those observed in the reaction of *S*-ethyl-L-Cys (data not shown).

Rapid-Scanning Stopped-Flow Kinetic Studies of Tyrosine and 3-Fluorotyrosine. We have also examined the reactions of L-Tyr and 3-fluoro-L-Tyr in the absence and presence of 4-HP by rapid-scanning stopped-flow spectrophotometry. The results for the reaction of TPL with L-Tyr are shown in Figure 3A. There is rapid formation of a low-intensity quinonoid band at 502 nm, which is concomitant with a decrease in the external aldimine band at 418 nm, and a low-intensity absorbance increase is seen at ~338 nm (Figure 3B). These data were fit by global analysis, and a minimum of at least three exponentials is required to obtain an adequate fit of these data. The three-exponential fit is consistent with the individual single-wavelength data, which exhibit a single exponential for the absorbance increase at 502 nm, biphasic kinetics at 418 nm, the fastest of which agrees with the rate constant at 502 nm, and biphasic kinetics at 338 nm, the fast phase matching the slow phase at 418 nm. The fastest phase corresponds to a decrease in the magnitude of the external aldimine band at 418 nm and an increase in the magnitude of the quinonoid band at 502 nm, with a k_{obs} of $\sim 70 \pm 5$ s^{-1}. This is in good agreement with our previous results (*25*). In the second phase, there is little change in the

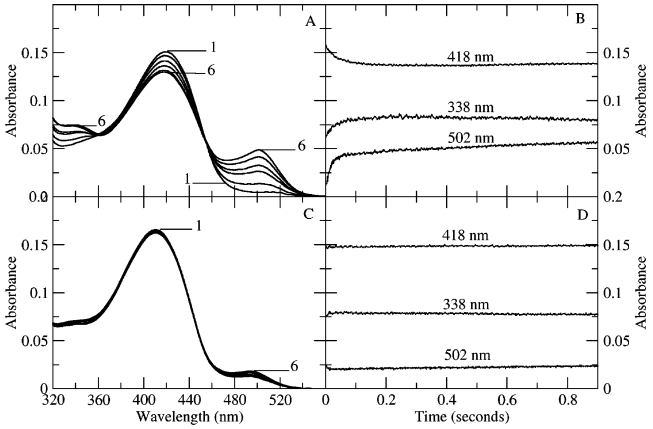

FIGURE 3: Rapid-scanning stopped-flow spectra of the reaction of TPL with L-Tyr. (A) Reaction of TPL with 2 mM L-Tyr in 0.05 M potassium phosphate (pH 8). The scans are shown at (1) 0.002, (2) 0.007, (3) 0.023, (4) 0.045, (5) 0.358, and (6) 0.803 s. (B) Time courses for the reaction shown in panel A at 338, 418, and 502 nm. (C) Reaction of TPL with 2 mM [α-^{2}H]-L-Tyr in 0.05 M potassium phosphate (pH 8). The scans are shown at (1) 0.002, (2) 0.292, (3) 0.582, (4) 0.872, (5) 1.452, and (6) 2.612 s. (D) Time courses for the reaction shown in panel C at 338, 418, and 502 nm.

502 nm band, but there is a decrease at 418 nm, which is concomitant with an increase at 338 nm, with a k_{obs} of 12 ± 2 s^{-1}. The slowest phase results in an increase in the magnitude of the quinonoid absorption band at 502 nm, with a rate constant of 1 ± 0.1 s^{-1}. The reaction of [α-^{2}H]-L-Tyr is similar to that of L-Tyr (Figure 3C), but the amplitudes and rates for formation of intermediates are dramatically reduced. The small amplitudes (Figure 3D) make it difficult to obtain the rate constants for the reaction with accuracy. The rate constant for quinonoid intermediate formation from [α-^{2}H]-L-Tyr is 20 ± 5 s^{-1}, so there is an apparent primary kinetic isotope effect of ~3.5 for the removal of the α-proton.

When 4-HP is included in the reaction of L-Tyr, in addition to absorption bands with maxima at 502 and 418 nm, there is also a more prominent peak at 338 nm (Figure 4A). As described above with L-Tyr, the reaction requires a minimum of three exponential processes to obtain a reasonable fit. The SVD spectra for the reaction of TPL with L-Tyr and 4-HP obtained from global fitting are shown in Figure 5A. Comparison of the residuals from the fits with two or three exponentials clearly shows that three exponentials are required to fit that data (compare the solid line and dashed line in Figure 5B). The fast phase exhibits an increase in absorbance at 502 nm and a decrease at 418 nm (Figure 5A, dotted line), with a k_{obs} of 64 ± 10 s^{-1}. The second phase exhibits a decrease in absorbance at 418 nm, an absorbance increase at 340 nm, and only a small change at 502 nm (Figure 5A, dashed line), with a k_{obs} of 7.3 ± 1 s^{-1}. The third phase is associated with an absorbance decrease at both 502 and 418 nm and a further absorbance increase at 338 nm (Figure 5A, dashed and dotted line), with a k_{obs} of 1.2 ± 0.2 s^{-1}. There is a good isosbestic point at 363 nm during the conversion of the 502 nm intermediate to the 338 nm species (Figure 4A). The reaction of [α-^{2}H]-L-Tyr in the presence of 4-HP also shows the formation of the 338 nm species (Figure 4C). Because of the low amplitude of the reaction at 502 nm, it is very difficult to obtain accurate rate constants for the first and second phases of the reaction. The rate constant for the third phase is 0.5 ± 0.1 s^{-1}. Thus, there

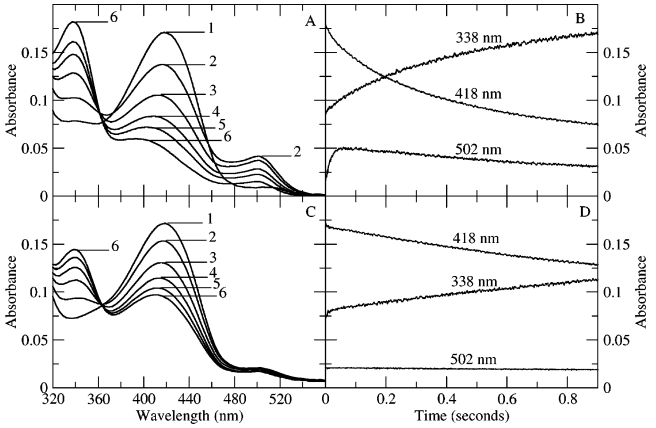

FIGURE 4: Rapid-scanning stopped-flow spectra of the reaction of TPL with L-Tyr in the presence of 4-HP. (A) Reaction of TPL with 2 mM L-Tyr and 5 mM 4-HP in 0.05 M potassium phosphate (pH 8). The scans are shown at (1) 0.002, (2) 0.095, (3) 0.292, (4) 0.582, (5) 0.872, and (6) 2.03 s. (B) Time courses for the reactions shown in panel A at 338, 418, and 502 nm. (C) Reaction of [α-^{2}H]-L-Tyr with 2 mM L-Tyr and 5 mM 4-HP in 0.05 M potassium phosphate (pH 8). The scans are shown at (1) 0.002, (2) 0.289, (3) 0.867, (4) 1.445, (5) 2.023, and (6) 2.60 s. (D) Time courses for the reactions shown in panel C at 338, 418, and 502 nm.

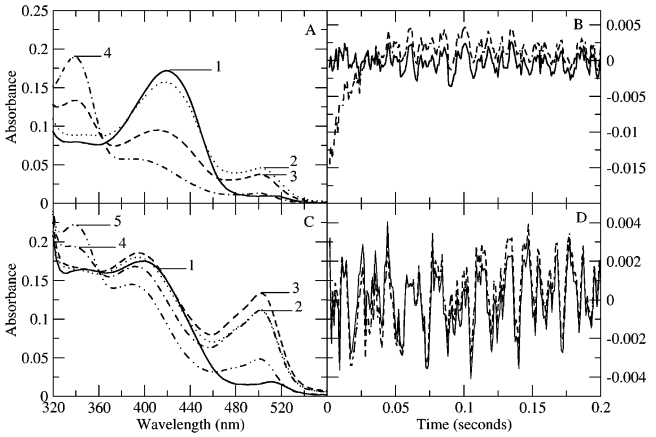

FIGURE 5: SVD spectra for the reactions of TPL with L-Tyr and 3-F-L-Tyr together with 4-HP. (A) Reaction of L-Tyr. (B) Residuals from global fits of the spectra. The solid line is for three exponentials and the dashed line for two exponentials. (C) Reaction of 3-F-Tyr. (D) Residuals from global fits of the spectra. The solid line is for four exponentials and the dashed line for three exponentials.

is a kinetic isotope effect of ~2.4 on the formation of the 338 nm intermediate from [α-^{2}H]-L-Tyr.

In the reaction of TPL with 3-fluoro-L-Tyr and other 3-halotyrosines, the spectra are similar to those obtained with tyrosine, but a more intense absorption peak is formed at 505 nm (data not shown). The rate constants for quinonoid intermediate formation are decreased for 3-Cl-, 3-Br-, and 3-I-substituted L-Tyrs, compared to those for L-Tyr and 3-F-L-Tyr (Table 2). As observed with L-Tyr, addition of 4-HP to reactions of 3-F-L-Tyr results in the formation of a new band at 338 nm (Figure 6A). In contrast to the reaction of L-Tyr, which has three phases, the reaction of 3-F-L-Tyr in the presence of 4-HP requires at least four exponential processes. This is due to the biphasic nature of the absorbance increase at 502 nm for 3-F-L-Tyr, in contrast to the monophasic course of the absorbance increase at 502 nm for L-Tyr. The corresponding SVD spectra for the reaction of TPL with 3-F-L-Tyr and 4-HP are shown in Figure 5C.

Table 2: Rate Constants for Quinonoid Intermediate Formation from 3-Halo-L-tyrosines

3-halo-L-Tyr	K_d (mM)	k_f (s^{-1})	k_r (s^{-1})	$k_f + k_r$
fluoro	0.8[a,b]	139.7[a,b]	6.9[a,b]	20.0[c]
chloro	0.23 ± 0.04	5.7 ± 0.2	4.4 ± 0.3	10.1
bromo	0.62 ± 0.18	6.7 ± 0.5	5.1 ± 0.5	11.8
iodo	0.65 ± 0.1	5.2 ± 0.2	5.4 ± 0.1	10.6

[a] Data taken from ref *18*. [b] Fast phase. [c] Slow phase.

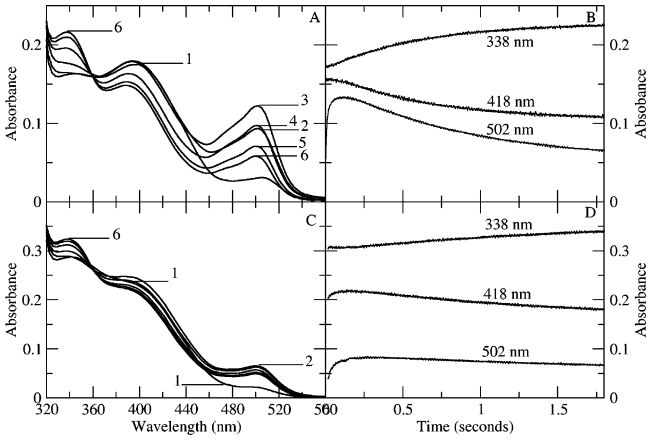

FIGURE 6: Rapid-scanning stopped-flow spectra of the reaction of TPL with 3-F-L-Tyr in the presence of 4-HP. (A) Reaction of TPL with 10 mM 3-F-L-Tyr and 5 mM 4-HP in 0.05 M potassium phosphate (pH 8). The scans are shown at (1) 0.002, (2) 0.012, (3) 0.174, (4) 0.528, (5) 1.13, and (6) 1.71 s. (B) Time courses for the reactions shown in panel A at 338, 418, and 502 nm. (C) Reaction of TPL with 10 mM [α-^{2}H]-3-F-L-Tyr and 5 mM 4-HP in 0.05 M potassium phosphate (pH 8). The scans are shown at (1) 0.002, (2) 0.204, (3) 0.570, (4) 1.15, (5) 1.53, and (6) 1.92 s. (D) Time courses for the reactions shown in panel C at 338, 418, and 502 nm.

In this case, the residuals are similar for three- and four-exponential fits (Figure 5D). However, the overall standard deviation is lower for the fit to four exponentials, and the single-wavelength data at 502 nm require two exponentials to fit the increasing absorbance phase, as mentioned above. Thus, the four-exponential fit is most consistent with all the data. The fastest phase of the reaction, which exhibits an absorbance increase at 505 nm (Figure 5C, dotted line), has a k_{obs} of 140 ± 20 s^{-1}, in good agreement with our previous results (*18*). The second phase of the reaction has a smaller amplitude but results in an additional absorbance increase at 505 nm (Figure 5C, dashed line), with a k_{obs} of 20 ± 4 s^{-1}. The third phase of the reaction shows an absorbance decrease at 420 nm and an increase at 338 nm, without much change at 505 nm (Figure 5C, dashed and dotted line), with a k_{obs} of 4 ± 1 s^{-1}. The slowest phase of the reaction is associated with an absorbance decrease at 505 and 420 nm and an absorbance increase at 338 nm (Figure 5C, dashed and double dotted line), with a k_{obs} of 1.4 ± 0.4 s^{-1}. When [α-^{2}H]-3-F-L-Tyr is used in the reaction with TPL and 4-HP, the rates and amplitudes are markedly decreased (Figure 6C). The fast phase has a k_{obs} of 48 ± 10 s^{-1}, so there is an apparent kinetic isotope effect of 2.9 on the fast phase of formation of the quinonoid intermediate. Previously, we reported an isotope effect of 6.0 on the intrinsic rate constant for quinonoid intermediate formation from 3-F-L-Tyr (*18*). The second phase of quinonoid intermediate formation exhibits a k_{obs} of 8.8 ± 1 s^{-1}, so there is also a kinetic isotope effect of 2.3 on this process. The third phase of the reaction

Table 3: Pre-Steady-State Kinetic Parameters for the Reaction of L-Tyr and 3-F-L-Tyr with TPL

substrate	$1/\tau_1$ (s^{-1})	$1/\tau_2$ (s^{-1})	$1/\tau_3$ (s^{-1})	$1/\tau_4$ (s^{-1})
L-Tyr	64 ± 10	−	7.3 ± 1	1.2 ± 0.2
[α-^{2}H]-L-Tyr	nd[a]	−	nd[a]	0.5 ± 0.1 (2.4)
3-F-L-Tyr	140 ± 20	20 ± 4	4 ± 1	1.4 ± 0.4
[α-^{2}H]-3-F-L-Tyr	48 ± 10 (2.9)	8.8 ± 1 (2.3)	3.6 ± 0.7	0.6 ± 0.1 (2.3)

[a] Not determined.

has a k_{obs} of 3.6 ± 0.7 s^{-1}, so it does not appear to be influenced by the deuterium substitution. The slowest phase of the reaction of [α-^{2}H]-3-F-L-Tyr has a k_{obs} of 0.60 ± 0.1 s^{-1}, so it exhibits a kinetic isotope effect of 2.3. The rate constants for the reactions of L-Tyr and 3-F-L-Tyr are summarized in Table 3.

DISCUSSION

α-Aminoacrylate intermediates are often proposed as intermediates in the reactions of PLP-dependent enzymes. These structures, bound as Schiff bases to the PLP cofactor, can serve as intermediates in either *β*-elimination or *β*-substitution reactions catalyzed by these enzymes. α-Aminoacrylates have been observed spectroscopically in the reactions of tryptophan synthase (*26*−*30*) and *O*-acetylserine sulfhydrylase (*31*−*34*), both of which catalyze *β*-substitution reactions. In the latter enzymes, the α-aminoacrylate structures are relatively stable in the absence of a nucleophilic substrate. In contrast, in the reaction of Trpase, which performs a *β*-elimination reaction, an α-aminoacrylate intermediate could be observed only in the presence of benzimidazole, an analogue of indole which is an uncompetitive inhibitor that binds to the α-aminoacrylate and inhibits its hydrolysis (*35*). TPL is highly homologous to Trpase and catalyzes a similar *β*-elimination reaction, which is also expected to proceed via an α-aminoacrylate species. However, there has been no previous direct observation of an α-aminoacrylate intermediate in the reaction of TPL. We postulated that a non-nucleophilic analogue of phenol, one of the products of TPL, would bind to the α-aminoacrylate and allow for its direct observation by rapid-scanning stopped-flow spectrophotometry.

Previously, we examined the binding of phenol and analogues, pyridine-*N*-oxide and 4-HP, to TPL complexes of L-alanine and D-alanine (*6*). While phenol selectively binds to the external aldimine complexes of L-alanine and D-alanine, both pyridine *N*-oxide and 4-HP were found to bind selectively to the quinonoid intermediates of L-alanine and D-alanine (*6*). Thus, we thought that 4-HP, a non-nucleophilic analogue of phenol, may bind preferentially to the α-aminoacrylate intermediate of TPL and stabilize it to allow for its observation. Rapid-scanning stopped-flow spectrophotometric studies of the reaction of TPL with *S*-ethyl-L-cysteine in the presence of 4-HP confirmed our expectation (Figure 1C). A new absorption peak, with a maximum at 338 nm, is observed when 5 mM 4-HP is added to the reaction mixture. α-Aminoacrylate intermediates seen in the reactions of tryptophan synthase (*26*−*30*) and *O*-acetyl-L-serine sulfhydrylase (*31*−*34*) exhibit absorption peaks at ∼350 and ∼460 nm. The protonation state of the α-aminoacrylate Schiff base nitrogen appears to affect the position of the absorption maximum. The peak at ∼350 nm in the spectrum of tryptophan synthase complexes with L-Ser was proposed to be the α-aminoacrylate, unprotonated on the Schiff base nitrogen, and the 460 nm peak was assigned to the protonated form (*36*). Like TPL, Trpase from *E. coli* forms an α-aminoacrylate with a maximum at 345 nm (*35*), suggesting that both TPL and Trpase preferentially form the unprotonated α-aminoacrylate.

Scheme 2

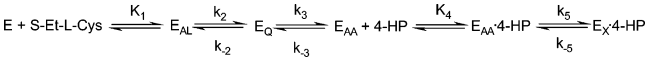

The decay of the quinonoid intermediate from *S*-ethyl-L-cysteine to form the α-aminoacrylate in the presence of 4-HP was found to be biphasic. The fast phase shows a hyperbolic decrease in rate with 4-HP concentration, while the slow phase shows a hyperbolic increase in rate with 4-HP concentration (Figure 2). These data are consistent with a mechanism involving rapid binding of 4-HP to the aminoacrylate intermediate, followed by a slower relaxation, as shown in Scheme 2. In this mechanism, the first step is formation of the external aldimine of *S*-ethyl-L-Cys (E_{AL}), followed by formation of the quinonoid intermediate (E_Q). The rate constant for the first step is given by eq 4.

$$k_{obs} = 1/\tau_1 = k_2[S\text{-ethyl-L-Cys}]/(K_1 + [S\text{-ethyl-L-Cys}]) + k_{-2} \quad (4)$$

The rate constant for this relaxation is independent of 4-HP concentration, as predicted by eq 4. Thus, 4-HP does not appear to bind directly to the quinonoid intermediate, in contrast to our earlier work with alanine, or if it binds, it does not affect the kinetics. The second phase of the reaction results from the relaxation between the quinonoid intermediate (E_Q in Scheme 2) and the aminoacrylate intermediate (E_{AA}). The rate constant for this phase, based on Scheme 2, is given by eq 5.

$$k_{obs} = 1/\tau_2 = k_{-3}K_4/(K_4 + [\text{4-HP}]) + k_3 \quad (5)$$

Fitting the data in Figure 2B (●) to eq 5 gives the following constants for 4-HP: $k_3 = 4.0 \pm 0.7$ s^{-1}, $k_{-3} = 18.2 \pm 2.1$ s^{-1}, and $K_4 = 0.9 \pm 0.4$ mM. The third phase results from the relaxation between E_{AA}·4-HP and another complex, E_X·4-HP. The apparent rate constant for this phase is given by eq 6.

$$k_{obs} = 1/\tau_3 = k_5[\text{4-HP}]/(K_4 + [\text{4-HP}]) + k_{-5} \quad (6)$$

The rate constants and binding constant for this reaction were determined by fitting the concentration-dependent data [Figure 2B (○)] to eq 6. The result of the fit gives the following constants for 4-HP: $k_5 = 2.6 \pm 0.2$ s^{-1}, $k_{-5} = 0.3 \pm 0.04$ s^{-1}, and $K_4 = 1.1 \pm 0.2$ mM. The values of K_4 obtained by fitting the data from the second and third phases are in good agreement.

The progress curves of the reaction of *S*-methyl-L-Cys at 505 nm also require three exponentials to produce a good fit. As with *S*-ethyl-L-Cys, the rate constant for the first phase, which is formation of the quinonoid intermediate, is independent of 4-HP concentration. However, in contrast to the results obtained with *S*-ethyl-L-cysteine, the rate constant for the second phase shows no significant change with an increase in 4-HP concentration. These data imply that the

reaction between E_Q and E_{AA} is not readily reversible (i.e., $k_{-3} \approx 0$) with methanethiol as the leaving group or nucleophile, possibly because of weak binding of methanethiol. As with *S*-ethyl-L-cysteine, the rate constant for the third phase exhibits an increase with a hyperbolic dependence on 4-HP concentration.

What is the structure of E_X? This species is formed from the α-aminoacrylate with a rate constant similar to k_{cat} for the steady-state reaction. However, it is possible that 4-HP affects the rate constant for E_X formation. In the *β*-elimination reaction, α-aminoacrylate is an intermediate, which results in the formation of ammonium pyruvate. It has been shown that the pyruvate is formed stereospecifically and that protonation of the *β*-carbon of the α-aminoacrylate occurs from the same face as the elimination (*2*). Thus, it is possible that E_X is an iminopyruvate complex, possibly bound as a *gem*-diamine (Scheme 1). A *gem*-diamine PLP complex would be expected to exhibit a λ_{max} at 325−330 nm, which would overlap with the spectrum of the α-aminoacrylate intermediate. It is also possible that E_X is a dead-end species not in the reaction path.

L-Tyr and 3-F-L-Tyr also form intermediates absorbing at 338 nm in the presence of 4-HP (Figures 4 and 6). Thus, an α-aminoacrylate Schiff base with PLP is also an intermediate in the reaction of L-Tyr and 3-F-L-Tyr. The rate constant for the formation of these α-aminoacrylates is quite slow and comparable to the values of k_{cat} for these substrates, ∼1−2 s^{-1} (*18*). Thus, it is likely that the elimination reaction is at least partially rate-limiting in the steady state for L-Tyr and 3-F-L-Tyr. For the reactions of the α-deuterated substrates, there is a substantial isotope effect on the rate constant of formation of the quinonoid intermediates, as expected. We found an intrinsic primary isotope effect of 6.0 on quinonoid intermediate formation of 3-F-L-Tyr in previous studies (*18*). However, there are also significant kinetic isotope effects of ∼2−3 on the formation of the α-aminoacrylates from L-Tyr and 3-F-L-Tyr when α-deuterated substrates are used in the reaction (Table 3). This result is consistent with the internal return of the α-proton to the phenol leaving group. This was reported by Faleev et al. (*1*) and Palcic et al. (*2*), who found deuterium in the phenol produced from the reaction of [α-^{2}H]-L-Tyr. A similar result was found in previous work with Trpase, where there is a kinetic isotope effect of 3.0 on the formation of the aminoacrylate intermediate from [α-^{2}H]-L-Trp (*14*, *15*), and there is internal return of the α-proton to the indole leaving group (*37*). In previous work, we assessed the exchange of the α-proton of L-Phe and L-Met in D_2O and we found that the wash out is slow, with a rate of <3.1 s^{-1} (*38*), comparable to the observed rate constants for α-aminoacrylate formation, so it is reasonable that internal return of the α-proton to the phenol leaving group can occur. Previous steady-state kinetic studies found primary kinetic isotope effects on k_{cat} and k_{cat}/K_m of ∼3 for both L-Tyr and 3-F-L-Tyr (*8*, *18*). In light of these results, these isotope effects are likely to be a reflection of the isotope effect on the slow elimination step, rather than the much faster formation of the quinonoid intermediate. The observation that the isotope effect is observed for α-aminoacrylate intermediate formation suggests that $C_\beta-C_1$ bond cleavage is concerted with protonation. Multiple isotope effect studies with Trpase provided evidence for a similar concerted SE_2 mechanism in the elimination of indole (*15*). Alternatively, the proton transfer to C_1 is slow and $C_\beta-C_1$ bond cleavage fast, if the mechanism is stepwise.

S-Alkyl-L-cysteines, L-Tyr, and 3-F-L-Tyr form low concentrations of intermediates absorbing at ∼340 nm without 4-HP present (Figures 1A and 3A). With *S*-ethyl-L-Cys, formation of this intermediate is concomitant with a decrease in the absorbance at 504 nm (Figure 1B). Furthermore, the rate constant for the formation of the 340 nm peak is identical to that of the decrease in the 504 nm peak. These results suggest that this intermediate is in fact an α-aminoacrylate. In contrast, in the reactions of L-Tyr and 3-F-L-Tyr, the magnitude of the external aldimine band at 420 nm decreases, while there is little change in the quinonoid band at 502 nm (Figure 3A). Also, there does not seem to be an isotope effect on the formation of this intermediate from the α-^{2}H-labeled substrate for 3-F-L-Tyr (Table 3). Thus, it seems unlikely that this species is the α-aminoacrylate resulting from the elimination in the case of L-Tyr and 3-F-L-Tyr. It is possible that this 340 nm absorption arises from a ketimine complex resulting from protonation of the quinonoid intermediate at C-4′. The abortive transamination of amino acids by TPL has been described previously (*39*). Alternatively, the 340 nm species could be an enolimine tautomer of the external aldimine, formed by a change in the polarity of the active site with expulsion of water.

It is also interesting that the formation of the quinonoid intermediate from 3-F-L-Tyr is biphasic, while that from L-Tyr is a single exponential. Both phases of the reaction with 3-F-L-Tyr are sensitive to isotopic substitution at the α-carbon, so both of them appear to be due to abstraction of the α-proton. Under experimental conditions, at pH 8.0, L-Tyr exists predominantly in a normal zwitterion form, while with 3-F-Tyr, which has a lower pK_a value for the phenol (8.7, compared to 10.0), significant amounts of the zwitterionic and phenolate anionic forms are present in the reaction mixture. We have shown previously (*40*) that for ring-substituted tyrosines, both zwitterionic and anionic forms of substrates can be bound and catalytically transformed by TPL. Hence, it seemed possible that the two phases might result from reaction of the different ionic forms of 3-F-L-Tyr. On the other hand, we have previously reported data consistent with steric effects in the interactions of TPL and Trpase with fluorotyrosines (*41*), and thus, a steric effect of F is possible. Rotamers of the fluorophenol ring of 3-F-L-Tyr oriented differently in the active site might react with different rates. To shed light on these questions, we examined the interaction of TPL with 3-Cl-, 3-Br-, and 3-I-tyrosines. For these substrates, comparable amounts of zwitterionic and phenolate anionic forms should be present (the pK_as are 8.5, 8.4, and 8.5, respectively), while the steric parameters of these ring substituents are much greater than those of F, increasing in the following order: Cl < Br < I. In constrast to 3-F-L-Tyr, we have found that for all three halotyrosine substrates the formation of quinonoid intermediates is monophasic, with the concentration dependencies described by eq 2. The respective kinetic parameters are listed in Table 2. We may conclude, therefore, that the two phases observed for the reaction of 3-F-Tyr probably are not associated with different ionic forms of the substrate. Thus, it is likely that the two rates observed with 3-F-L-Tyr result from reaction of different rotamers of the fluorophenol ring, which orient the fluorine substituent in a different location. On the other

hand, the kinetic parameters observed for 3-Cl-, 3-Br-, and 3-I-L-tyrosines are very similar (Table 2), despite very different steric parameters for these substituents. It seems likely that the situation in the active site is such that, depending on the orientation of the phenol ring, one rotamer can readily accommodate F, but not larger halogens, whereas the other rotamer allows F or much larger Cl, Br, and I substituents to be accommodated, but with a slower reaction rate. In addition, the fast phase of quinonoid intermediate formation with 3-F-L-Tyr is considerably faster than that with L-Tyr (Table 3). Since hydrogen bonding by aryl fluorine is unlikely, this difference likely is due to favorable van der Waals interactions. The phenol ring of the substrate would have to undergo considerable movement as the quinonoid intermediate is formed since there is rehybridization of the α-carbon from sp^3 to sp^2 (*41*), and thus, it is reasonable to expect ring substituents to affect the transition state for α-deprotonation. The observed effects of substituents should reflect, consequently, the decrease in the number of possible rotamers with the increase in the steric parameters of the substituents. The monotonic decrease in the α-proton lability in the following order agrees with this interpretation: 64 s^{-1} (Tyr) > 20 s^{-1} (slow phase for 3-F-Tyr reaction) > 10−12 ($k_f + k_r$ for 3-Cl-, 3-Br-, and 3-I-L-tyrosines).

Conclusions. α-Aminoacrylate intermediates do not accumulate to a significant extent in the steady state of TPL reactions. 4-HP binds to and stabilizes α-aminoacrylates of TPL and allows for their detection in the reactions of *S*-alkyl-L-Cys, L-Tyr, and 3-F-L-Tyr. Elimination and pyruvate formation are at least partially rate liming in the reactions catalyzed by TPL.

REFERENCES

1. Faleev, N. G., Lyubarev, A. E., Martinkova, N. S., and Belikov, V. M. (1983) Mechanism and stereochemistry of α,β-elimination of L-tyrosine catalysed by tyrosine phenol-lyase, *Enzyme Microb. Technol. 5*, 219−224.
2. Palcic, M. M., Shen, S. J., Schleicher, E., Kumagai, H., Sawada, H., Yamada, H., and Floss, H. G. (1987) Stereochemistry and mechanism of reactions catalyzed by tyrosine phenol-lyase from *Escherichia intermedia*, *Z. Naturforsch. 42C*, 307−318.
3. Kumagai, H., Yamada, H., Matsui, H., Ohkishi, H., and Ogata, K. (1970) Tyrosine Phenol Lyase. I. Purification, Crystallization, and Properties, *J. Biol. Chem. 245*, 1767−1772.
4. Phillips, R. S. (1987) Reactions of *O*-Acyl-L-serines with Tryptophanase, Tyrosine Phenol-lyase and Tryptophan Synthase, *Arch. Biochem. Biophys. 256*, 302−310.
5. Kumagai, H., Kashima, N., and Yamada, H. (1970b) Racemization of D- or L-alanine by crystalline tyrosine phenol-lyase from *Escherichia intermedia*, *Biochem. Biophys. Res. Commun. 39*, 796−801.
6. Chen, H. Y., and Phillips, R. S. (1993) Binding of Phenol and Analogues to Alanine Complexes of Tyrosine Phenol-lyase from *Citrobacter freundii*: Implications for the Mechanism of β-Elimination and Alanine Racemization, *Biochemistry 32*, 11591−11599.
7. Muro, T., Nakatani, H., Hiromi, K., Kumagai, H., and Yamada, H. (1978) Elementary Processes in the Interaction of Tyrosine Phenol Lyase with Inhibitors and Substrate, *J. Biochem. 84*, 633−640.
8. Kiick, D. M., and Phillips, R. S. (1988) Mechanistic Deductions from Kinetic Isotope Effects and pH Studies of Pyridoxal Phosphate-dependent Carbon−carbon Lyases: *Erwinia herbicola* and *Citrobacter freundii* Tyrosine Phenol-lyase, *Biochemistry 27*, 7339−7344.
9. Sundararaju, B., Antson, A.-A., Phillips, R. S., Demidkina, T. V., Barbolina, M. V., Gollnick, P., Dodson, G. G., and Wilson, K. S. (1997) The Crystal Structure of *Citrobacter freundii* Tyrosine Phenol-lyase Complexed with 3-(4′-Hydroxyphenyl)propionic Acid, Together with Site-directed Mutagenesis and Kinetic Analysis, Demonstrates that Arginine-381 is Required for Substrate Specificity, *Biochemistry 36*, 6502−6510.
10. Antson, A. A., Demidkina, T. V., Gollnick, P., Dauter, Z., Von Tersch, R. L., Long, J., Berezhnoy, S. N., Phillips, R. S., Wilson, K. S., and Harutyunyan, E. H. (1993) The Three-dimensional Structure of Tyrosine Phenol-lyase, *Biochemistry 32*, 4195−4206.
11. Isupov, M. N., Antson, A. A., Dodson, E. J., Dodson, G. G., Dementieva, I. S., Zakomirdina, L. N., Wilson, K. S., Dauter, Z., Lebedev, A. A., and Harutyunyan, E. H. (1998) Crystal structure of Tryptophanase, *J. Mol. Biol. 276*, 603−623.
12. Kiick, D. M., and Phillips, R. S. (1988) Mechanistic Deductions from Multiple Kinetic and Solvent Isotope Effects and pH Studies of Pyridoxal Phosphate-Dependent Carbon−carbon Lyases: *Escherichia coli* Tryptophan Indole-lyase, *Biochemistry 27*, 7333−7338.
13. Lee, M., and Phillips, R. S. (1995) The Mechanism of *Escherichia coli* Tryptophan Indole-lyase: Substituent Effects on Steady-state and Pre-steady-state Kinetic Parameters for Aryl-substituted Tryptophan Derivatives, *Biol. Med. Chem. 3*, 195−205.
14. Sloan, M. S., and Phillips, R. S. (1996) Effects of α-Deuteration and of Aza and Thia Analogs of L-Tryptophan on Formation of Intermediates in the Reaction of *Escherichia coli* Tryptophan Indole-lyase, *Biochemistry 35*, 16165−16173.
15. Phillips, R. S., Sundararju, B., and Faleev, N. G. (2000) Proton Transfer and Carbon−Carbon Bond Cleavage in the Elimination of Indole Catalyzed by *Escherichia coli* Tryptophan Indole-lyase, *J. Am. Chem. Soc. 122*, 1008−1114.
16. Dua, R. K., Taylor, E. W., and Phillips, R. S. (1993) S-Aryl-L-cysteine S,S-Dioxides: Design and Evaluation of a New Class of Mechanism Based Inhibitors of Kynureninase, *J. Am. Chem. Soc. 115*, 1264−1270.
17. Von Tersch, R. L., Secundo, F., Phillips, R. S., and Newton, M. G. (1996) Preparation of Fluorinated Amino Acids with Tyrosine Phenol-lyase: Effects of fluorination on the reaction kinetics and mechanism of tyrosine phenol-lyase and tyrosine protein kinase Csk, *ACS Symp. Ser. 639*, 95−104.
18. Chen, H., Phillips, R. S., and Gollnick, P. (1995) Site-directed Mutagenesis of Histidine 343 to Alanine in *Citrobacter freundii* Tyrosine Phenol-lyase: Effects on the Kinetic Mechanism and Rate-determining Step, *Eur. J. Biochem. 229*, 540−549.
19. Morino, Y., and Snell, E. E. (1970) Tryptophanase (*Escherichia coli* B), *Methods Enzymol. 17A*, 439−446.
20. Cleland, W. W. (1979) Statistical Analysis of Enzyme Kinetic Data, *Methods Enzymol. 63*, 103−138.
21. Matheson, I. B. C. (1990) A critical comparison of least absolute deviation fitting (robust) and least-squares fitting: The importance of error distributions, *Comput. Chem. 14*, 49−57.
22. Durbin, J., and Watson, G. S. (1950) Testing for serial correlation in least squares regression. I, *Biometrika 37*, 409−428.
23. Fisher, H. F. (2005) Transient-state Kinetic Approach to Mechanisms of Enzymatic Catalysis, *Acc. Chem. Res. 38*, 157−166.
24. Strickland, S., Palmer, G., and Massey, V. (1975) Determination of dissociation constants and specific rate constants of enzyme−substrate (or protein−ligand) interactions from rapid reaction kinetic data, *J. Biol. Chem. 250*, 4048−4052.
25. Sundararaju, B., Chen, H., Shillcutt, S., and Phillips, R. S. (2000) The Role of Glutamic Acid-69 in the Activation of *Citrobacter freundii* Tyrosine Phenol-lyase by Monovalent Cations, *Biochemistry 39*, 8546−8555.
26. Lane, A. N., and Kirschner, K. (1983) The catalytic mechanism of tryptophan synthase from *Escherichia coli*. Kinetics of the reaction of indole with the enzyme−L-serine complexes, *Eur. J. Biochem. 129*, 571−582.
27. Drewe, W. F., and Dunn, M. F. (1986) Characterization of the reaction of L-serine and indole with *Escherichia coli* tryptophan synthase via rapid-scanning ultraviolet−visible spectroscopy, *Biochemistry 25*, 2494−2501.
28. Brzovic, P. S., Kayastha, A. M., Miles, E. W., and Dunn, M. F. (1992) Substitution of glutamic acid 109 by aspartic acid alters the substrate specificity and catalytic activity of the β-subunit in the tryptophan synthase bienzyme complex from *Salmonella typhimurium*, *Biochemistry 31*, 1180−1190.
29. Weber-Ban, E., Hur, O., Bagwell, C., Banik, U., Yang, L.-H., Miles, E. W., and Dunn, M. F. (2001) Investigation of allosteric linkages in the regulation of tryptophan synthase: The roles of salt bridges and monovalent cations probed by site-directed mutation, optical spectroscopy, and kinetics, *Biochemistry 40*, 3497−3511.

30. Cash, M. T., Miles, E. W., and Phillips, R. S. (2004) The Reaction of Indole with the Aminoacrylate Intermediate of *Salmonella typhimurium* Tryptophan Synthase: Observation of a Primary Kinetic Isotope Effect with 3-[^{2}H]-Indole, *Arch. Biochem. Biophys. 432*, 233−243.
31. Cook, P. F., and Wedding, R. T. (1976) A reaction mechanism from steady-state kinetic studies for O-acetylserine sulfhydrylase from *Salmonella typhimurium* LT-2, *J. Biol. Chem. 251*, 2023−2029.
32. Woehl, E. U., Tai, C. H., Dunn, M. F., and Cook, P. F. (1996) Formation of the α-aminoacrylate immediate limits the overall reaction catalyzed by O-acetylserine sulfhydrylase, *Biochemistry 35*, 4776−4783.
33. Cook, P. F., Tai, C. H., Hwang, C. C., Woehl, E. U., Dunn, M. F., and Schnackerz, K. D. (1996) Substitution of pyridoxal 5′-phosphate in the O-acetylserine sulfhydrylase from *Salmonella typhimurium* by cofactor analogs provides a test of the mechanism proposed for formation of the α-aminoacrylate intermediate, *J. Biol. Chem. 271*, 25842−25849.
34. Tai, C. H., Yoon, M. Y., Kim, S. K., Rege, V. D., Nalabolu, S. R., Kredich, N. M., Schnackerz, K. D., and Cook, P. F. (1998) Cysteine 42 is important for maintaining an integral active site for O-acetylserine sulfhydrylase resulting in the stabilization of the α-aminoacrylate intermediate, *Biochemistry 37*, 10597−10604.
35. Phillips, R. S. (1991) The Reaction of Indole and Benzimidazole with Amino Acid Complexes of *E. coli* Tryptophan Indole-lyase: Detection of a New Reaction Intermediate, *Biochemistry 30*, 5927−5934.
36. Hur, O., Niks, D., Casino, P., and Dunn, M. F. (2002) Proton Transfers in the β-Reaction Catalysed by Tryptophan Synthase, *Biochemistry 41*, 9991−10001.
37. Vederas, J. C., Schleicher, E., Tsai, M. D., and Floss, H. G. (1978) Stereochemistry and mechanism of reactions catalyzed by tryptophanase *Escherichia coli*, *J. Biol. Chem. 253*, 5350−5354.
38. Faleev, N. G., Demidkina, T. V., Tsvetikova, M. A., Phillips, R. S., and Yamskov, I. A. (2004) The Mechanism of α-Proton Isotope Exchange in Amino Acids Catalysed by Tyrosine Phenol-lyase, *Eur. J. Biochem. 271*, 4565−4571.
39. Demidkina, T. V., Myagkikh, I. V., and Azhayev, A. V. (1987) Transamination catalysed by tyrosine phenol-lyase from *Citrobacter intermedius*, *Eur. J. Biochem. 170*, 311−316.
40. Faleev, N. G., Axenova, O. V., Demidkina, T. V., and Phillips, R. S. (2003) The role of acidic dissociation of substrate's phenol group in the mechanism of tyrosine phenol lyase, *Biochim. Biophys. Acta 1647*, 260−265.
41. Phillips, R. S., Von Tersch, R. L., and Secundo, F. (1997) Effects of Tyrosine Ring Fluorination on Rates and Equilibria of Formation of Intermediates in the Reactions of Carbon−carbon Lyases, *Eur. J. Biochem. 244*, 658−663.

BI060561O